Title
CROSSED MOLECULAR BEAM STUDIES ON THE INTERACTION POTENTIAL FOR F(2p) + Xe(ls)

Author
Becker, C.

Publication Date
1978-05-01

Submitted to Journal of Chemical Physics

LBL-7674
Preprint

c.2

CROSSED MOLECULAR BEAM STUDIES ON THE INTERACTION POTENTIAL FOR $F(^2P) + Xe(^1S)$

C. Becker, P. Casavecchia, and Y. T. Lee

May 1978

Prepared for the U. S. Department of Energy
under Contract W-7405-ENG-48

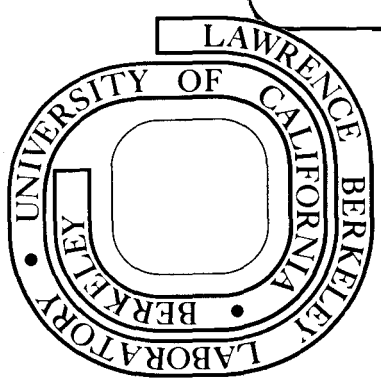

LBL-7674

c.2

DISCLAIMER

LBL-7674

CROSSED MOLECULAR BEAM STUDIES ON THE INTERACTION POTENTIAL FOR $F(^2P) + Xe(^1S)$

C. Becker, P. Casavecchia*, and Y. T. Lee†

Materials and Molecular Research Division
Lawrence Berkeley Laboratory
and Department of Chemistry
University of California
Berkeley, California 94720

ABSTRACT

For the evaluation of ground state XeF interaction potential, angular distributions of F atoms scattered off Xe were measured in crossed molecular beam experiments at collision energies of 2.11, 10.5, and 13.9 kcal/mole. F atoms produced by thermal dissociation of F_2 at 700°C in a supersonic expansion using rare gas carriers contain ~78% F ($^2P_{3/2}$) ground state and ~22% F ($^2P_{1/2}$) spin-orbit excited state. Consequently, three electronic states, $X\,\frac{1}{2}$, $I\,\frac{3}{2}$ emerging from the $^2P_{3/2} + {}^1S_0$ asymptote, and $II\,\frac{1}{2}$ from the $^2P_{1/2} + {}^1S_0$ asymptote are involved in the scattering. A simple elastic approximation, neglecting inter-state coupling, is used for the calculation of differential scattering cross sections in the evaluation of interaction potentials. Experimental results are found corroborating the spectroscopically derived potential of Tellinghuisen et al. (ε = 3.359 kcal/mole, r_m = 2.293 Å) for $V_{X\,\frac{1}{2}}(r)$, and the conclusion that $V_{I\,\frac{3}{2}}(r)$ and $V_{II\,\frac{1}{2}}(r)$ are in close resemblance to the ground state Ne + Xe interaction potential.

INTRODUCTION

Recently much work has focused on diatomic rare-gas halide molecules because they comprise a new class of lasers in the near to vacuum ultraviolet region. Spontaneous emission and laser action from many of the rare gas-halide (RG-X) combinations have now been reported.[1] The ground state RG-X interactions themselves are also of fundamental chemical interest. The lack of detailed information on RG-X interaction potentials, in the past, made it difficult to evaluate the theoretical understanding of the termolecular recombination of halogen atoms in a rare gas environment. The lasing excited states seem rather well described by an ionic model,[2] and the effect of the spin-orbit interaction amongst these states has been clearly detailed in ab initio calculations by Hay and Dunning.[3] The lower electronic manifold interactions ($^2P_{3/2,1/2} + {}^1S_0$) are not as simply described. Usually the potential energy curves are said to exhibit repulsive or van der Waals character;[4] yet the two curves arising from the energetically lower $^2P_{3/2} + {}^1S_0$ asymptote are significantly split.[3,4] This splitting can be explained in simple terms by the amount of electron overlap due to the different orientations of the halogen p orbitals. However it is also thought that for some systems (especially XeF and XeCl) there may be significant charge transfer involved in the ground state binding. An indication of this fact comes from the observation of bound-bound emission in the XeF and XeCl spectra. Particular effort has been paid to the XeF system and the potential energy curves involved in the laser emission have been derived spectroscopically.[5,6]

The most detailed spectra contain rotational as well as vibrational structure affording an internuclear distance estimate in addition to the well depth for the ground state and two strongly fluorescing states.[5c]

Experiments involving the decomposition of $FXeOSO_2F$ and $XeF^+OsF_6^-$ suggested the processes occurred via XeF formation; an estimate of a XeF binding energy of ~20 kcal/mole has been made.[7] Support for an estimate of ~10 kcal/mole came from studies suggesting a XeF role in the oxidation of NO and NO_2,[8] and H_2O[9] by XeF_2. Also the observation of XeF was reported in an electron spin resonance spectrum, the sample being a γ radiation damaged XeF_4 single crystal;[10] this study described the XeF as a σ-electron radical.

The XeF ground state, denoted $X^2\Sigma^+_{1/2}$ ($X\ \frac{1}{2}$) in Hund's case b (c) has attracted attention for several ab initio and semi-empirical calcalulations.[3b,4,11] Because of the large number of electrons involved, even with a "state of the art" calculation, none of the curves computed compare satisfactorily in the well region with the spectra derived potential of Tellinghuisen et al.[5c]

Consequently, in an effort to investigate the attractive well of the XeF ground state interaction potential, we have carried out differential cross section measurements for F ($^2P_{3/2,1/2}$) scattered off Xe ($^1S_0$) at three collision energies.

EXPERIMENTAL

The basic experimental technique has been described elsewhere in detail.[12] Supersonic beams of xenon and fluorine atoms seeded in a rare gas carrier are crossed at 90° in a collision chamber maintained at $\sim 3 \times 10^{-7}$ torr. Fluorine atoms are detected as a function of in plane scattering angle by a triply differentially pumped rotatable quadrupole mass spectrometer.

The fluorine atoms are produced by thermal dissociation of F_2 in a resistively heated nickel oven/nozzle (typically at ~700°C). Under normal operating temperature and F_2 partial pressure we estimated[13] and confirmed experimentally about equal flux or F and F_2 from the source. The signal at m/e 19 due to the dissociative ionization of scattered F_2 flux presented the greatest uncertainty in the ^{19}F atom scattering data. After several angular scans at m/e 19 (typically counting for 30 to 60 seconds at each angle) the intensity at m/e 38 was measured and compared over the same angular range. This comparison, combined with the estimated m/e 38:19 ratio for F_2 in the mass spectrometer allowed a subtraction of the F_2 contribution to obtain a corrected angular distribution of scattered F atoms as a function of laboratory scattering angle, $I(\Theta)$, for F + Xe.

The F_2^+/F^+ ratio for F_2 was measured as a function of oven temperature in a temperature range where no signficant dissociation takes place, and these values are extrapolated to the operation temperature. Because $I(\Theta)$ of F_2 for the F_2 + Xe scattering showed no oscillations at any observed angle, and had high intensity and large slope at small

angles, any resultant error in $I(\Theta)$ of F for F + Xe would be a skewing at angles less than ~10°. We estimate a maximum systematic error of ~10% based on the reproducibility of measured m/e 38:19 intensities. All reported $I(\Theta)$ are relative values.

The thermal F source at ~700°C contains the spin-orbit excited component $^2P_{1/2}$. Due to the 404 cm^{-1} splitting, the amount of electronic to translational relaxation in the supersonic expansion under present conditions is expected to be small; thus the F ($^2P_{1/2}$) contribution to the mixed beam is estimated by Boltzmann and degeneracy weights.

The three relative collisions energies, nominally 2.11, 10.5, 13.9 kcal/mole, were obtained with 99% Ar/1% F_2, 96.5% He/3% Kr/0.5% F_2, and 99% He/1% F_2 gas mixtures, respectively, from stagnation pressure of ~500 torr behind the nozzle at ~700°C. The pure Xe beam was kept at room temperature. Supersonic beam velocity peaks and distributions were measured by time-of-flight detection. Typical full width half maximum velocity spreads for F and Xe are both ~10%.

RESULTS AND ANALYSIS

The experimental data of $I(\Theta)$ for F + Xe at three collision energies is shown in Fig. 1 along with error bars representing ± one standard deviation. The nominal collision energies are also shown. The angular distribution at the lowest energy displays practically no oscillatory structure, whereas the two higher energy $I(\Theta)$ show a

low amplitude, slow oscillation with a faster oscillation superimposed. The physical interpretation of these $I(\theta)$ follow.

Inelastic cross sections in these experiments involving the electronic transition between F ($^2P_{3/2}$) and F ($^2P_{1/2}$) are expected to be much smaller than elastic cross sections because the spin-orbit splitting (Δ) constitutes an appreciable fraction of the relative collision energy (E_{rel}). The inefficiency of this electronic transition has been shown in a recent semiclassical calculation for F + Xe.[14] Therefore a simple elastic approximation is employed in the analysis of $I(\theta)$. In this model the total differential cross section is written as a sum of elastic differential cross sections $\sigma_{X\frac{1}{2}}(\theta)$, $\sigma_{I\frac{3}{2}}(\theta)$, and $\sigma_{II\frac{1}{2}}(\theta)$ for the three states $X\frac{1}{2}$, $I\frac{3}{2}$, and $II\frac{1}{2}$, where each elastic differential scattering cross section in the center of the mass coordinate system, $\sigma(\theta)$, is calculated from the associated single channel scattering[15] employing the corresponding spherically symmetric interaction potential given as a function of internuclear distance:

$$\sigma_{tot}(\theta) = \sigma_{X\frac{1}{2}}(\theta) + \sigma_{I\frac{3}{2}}(\theta) + a\sigma_{II\frac{1}{2}}(\theta) \quad . \qquad (1)$$

The factor a (=0.55) represents the 22% contribution of F ($^2P_{1/2}$) in the beam of F atoms. The $X\frac{1}{2}$ and $I\frac{3}{2}$ states correlate with the $^2P_{3/2} + {}^1S_0$ asymptote, while $II\frac{1}{2}$ correlates with $^2P_{1/2} + {}^1S_0$. $\frac{1}{2}$ and $\frac{3}{2}$ following X, I, and II are Ω quantum numbers; Ω is the projection of the total electronic angular momentum along the molecular axis.

This approximation should serve the useful purpose of evaluating interaction potentials. We note, however, that this approximation cannot account for the fast oscillations in $I(\Theta)$ which are believed to show perturbations in the elastic scattering due to non-adiabatic coupling between the three electronic states. This interpretation of the fast oscillations follows from the observation that the spacing of these oscillations is inversely proportional to the relative velocity.[16]

For the comparison of interaction potentials with the experimental $I(\Theta)$ we first use a flexible analytic form to describe the potentials for the calculation of $\sigma_{tot}(\Theta)$. The $\sigma_{tot}(\Theta)$ is then transformed into the laboratory coordinate system to give a calculated $I(\Theta)$, taking into account velocity and angular spread of the beams and spatial resolution of the detector. Comparison of calculated $I(\Theta)$ with experimental $I(\Theta)$ provides the basis for evaluation of the interaction potentials.

In the analysis of experimental results, the interaction potentials $V(r)$ are chosen to be the flexible piecewise analytic form Morse-Morse-switching function - van der Waals (MMSV) given here for reference:

$$f(x) = V(r)/\varepsilon \qquad x = r/r_m \tag{2}$$

$$\begin{aligned} f(x) &= \exp(2\beta_1(1-x)) - 2\exp(\beta_1(1-x)) , && 0 < x \leq 1 \\ &= \exp(2\beta_2(1-x)) - 2\exp(\beta_2(1-x)) \equiv M_2(x) && 1 < x \leq x_1 \\ &= SW(x) \cdot M_2(x) + (1 - SW(x)) \cdot W(x) && x_1 < x < x_2 \\ &= -C_{6r}x^{-6} - C_{8r}x^{-8} \equiv W(x) && x_2 \leq x < \infty \end{aligned}$$

and

$$SW(x) = \frac{1}{2}\left[\cos\left(\frac{\pi(x-x_1)}{(x_2-x_1)}\right) + 1\right] ,$$

where $C_{6r} = C_6/(\varepsilon r_m^6)$, and $C_{8r} = C_8/(\varepsilon r_m^8)$; ε and r_m are the depth and position of potential minimum. The usual cubic spline function is not used as it frequently produced a local maximum and minimum for the $V_{X\frac{1}{2}}(r)$ curve.

Since there is good reason to believe that the information on the attractive well of the $X\frac{1}{2}$ state derived from spectroscopic data by Tellinghuisen et al.[5c] is more reliable than other information available, the data analysis is started with a potential using their values of ε and r_m, and a morse β value is derived from the spectroscopic constant, ω_e.

In order to calculate the differential cross section, it is necessary to have information covering the full range of interaction potential probed at a given collision energy. This means in addition to the attractive portion of the potential curve, the high energy repulsive wall has to be added before comparison can be made. The repulsive wall of the potential is described by the inner morse function, characterized by β_1. Since the scattering data is the result of three interaction potentials, $X\frac{1}{2}$, $I\frac{3}{2}$, and $II\frac{1}{2}$, we also have to make reasonable estimates of the $I\frac{3}{2}$ and $II\frac{1}{2}$ potentials. Fortunately, data obtained at three different collision energies are sensitive to different regions and different states of interaction potentials; thus a very meaningful comparison between experimental $I(\Theta)$, and $I(\Theta)$ derived from a given set of potential curves is possible.

The $I\frac{3}{2}$ and $II\frac{1}{2}$ interaction potentials used in this work were assumed (a) to be very near the corresponding one electron richer rare gas pair Ne-Xe,[17] and (b) $V_{II\frac{1}{2}}(r) = V_{I\frac{3}{2}}(r) + \Delta$. Justification

is based on the closed shell-closed shell electronic configuration for the π symmetry, having the fully occupied fluorine p orbital along the internuclear axis (see reference 3b). Some slight adjustments to the corresponding Ne-Xe potential were made reflecting different polarizabilities[18,19] and electron spatial probabilities[20] going from Ne to F. Also the spin-orbit splitting, primarily associated with tightly bound core electrons, is approximated as constant over the range of internuclear distance probed.

The van der Waals C_6 constant is estimated by the Slater-Kirkwood formula[21] for effective number of electrons; polarizabilities were taken from the literature.[18,19] The C_6 constant of $I\frac{3}{2}$ is calculated to be larger than $X\frac{1}{2}$ state, reflecting its larger polarizability.[18] This implies a slow curve crossing for the $X\frac{1}{2}$ and $I\frac{3}{2}$ states at fairly large r. We note that the C_6 calculated for $X\frac{1}{2}$ has the long-range mixture of one-third $^2\Pi$ and two-thirds $^2\Sigma^+$ character,[3,14] while the $I\frac{3}{2}$ is purely $^2\Pi$. Though the $II\frac{1}{2}$ state asymptotically approaches two-thirds $^2\Pi$ and one-third $^2\Sigma^+$, we have used the C_6 of the $I\frac{3}{2}$ state in order to keep the same potential form for $I\frac{3}{2}$ and $II\frac{1}{2}$. This approximation should have no significant effect in the calculation and comparison of differential cross sections. The permanent quadrupole-induced dipole moment interaction, varying as R^{-8} at long range, contributes only a small fraction of the C_8 dispersion term,[22] which in turn has a small contribution compared to the C_6 term (dispersion only). The C_8 constant is estimated from the Ne-Xe C_8 constant.[19] Higher order constants are neglected due to their uncertainty and very small contribution.

With these initial assumptions for the $X\frac{1}{2}$ and $I\frac{3}{2}$, $II\frac{1}{2}$ potentials, the parameters ε, r_m, β_1, and β_2 were varied in an attempt to match the calculated with experimental $I(\Theta)$ at the three relative collision energies.

The use of the $V_{X\frac{1}{2}}(r)$ of Tellinghuisen et al. (i.e., $\varepsilon = 3.359$ kcal/mole, $r_m = 2.293$ Å, and $\beta_1 = \beta_2 = 7.47$) proved quite satisfactory, though a shift of a few degrees from the experimental data at two highest energies in the position of the slow oscillation maxima and minima in the $I(\Theta)$ was noted. Consequently, the $V_{X\frac{1}{2}}(r)$ derived here is modified slightly by altering β_1 and β_2 for a better $I(\Theta)$ fit, keeping ε and r_m the same. In adjusting β_1 and β_2, the width of the well was kept constant to within ~0.01 Å. It is not clear whether this slight improvement in the $X\frac{1}{2}$ potential is really significant, since the small difference is certainly within the limit of experimental uncertainties, especially the uncertainty in the experimentally determined collision energies. The original estimates for the $I\frac{3}{2}$ and $II\frac{1}{2}$ potentials were generally satisfactory and little change is made in deriving these potential parameters. The resulting potential parameters are listed in Table I.

$I(\Theta)$ sensitivity to the $V_{X\frac{1}{2}}(r)$ is quite good for the two highest energies, allowing an estimate of knowledge of the $V_{X\frac{1}{2}}(r)$ to within 5% by these methods. The sensitivity to the $V_{I\frac{3}{2}}(r)$ is not as good; its influence shows most clearly in $I(\Theta)$ fall-off behavior at small angles, especially for the lowest energy $I(\Theta)$. We assign a 15% measure of confidence to this potential near the attractive well.

Calculated I(Θ) from the derived potentials are plotted along with the data in Fig. 1. The calculated I(Θ) are scaled to the data by a constant scaling factor which is determined by the minimization of a chi(χ)-square goodness-of-fit measure. I(Θ) are averaged over the geometric resolution of the detector/beam arrangement in all calculations; one calculation at each nominal collision energy assumes mono-energetic beams (single Newton diagram) to display clearly the nature of the oscillations; the other calculated curves show the realistic effect of velocity averaging over 15 Newton diagrams. In the 10.5 and 13.9 kcal/mole I(Θ), the slow oscillations are rainbow and supernumerary rainbow oscillations produced by the $X\frac{1}{2}$ state. The 2.11 kcal/mole data show orbiting behavior for the $X\frac{1}{2}$ state.

In order to show both the sensitivity of this fitting procedure to given potentials, and how realistic other published XeF potentials are, we have presented additional velocity averaged calculations of I(Θ) in Fig. 2 derived from other potentials. The comparisons are made at low energy and one high relative collision energy. Dunning and Hay[3b] have presented potentials for all states of interest here. Using these as input, the I(Θ) are calculated and compared with the data. These I(Θ) are qualitatively in error, due to the absence of any appreciable well in the V(r). This is not unexpected from the type of calculation used by Dunning and Hay. Another recent XeF potential calculation[23] using a one-electron relativistic effective core potential does not significantly alter these potential curves.

As an example to show the sensitivity to the $I\frac{3}{2}$, $II\frac{1}{2}$ potentials, Fig. 2 also shows $I(\Theta)$ calculated from the $V_{X\frac{1}{2}}(r)$ of this work and the $V_{I\frac{1}{2},II\frac{3}{2}}(r)$ of Dunning and Hay. Significant deviation from experimental data is shown in the low energy $I(\Theta)$. Fig. 2 also depicts the deeper $X\frac{1}{2}$ potential put forth by Krauss and Liu,[11] combined with the $V_{I\frac{3}{2},II\frac{1}{2}}(r)$ derived in this work. This $X\frac{1}{2}$ potential is deep enough to produce orbiting at low energy, while at the high energy, the position of the rainbow maximum is severely displaced. All interaction potentials considered are shown in Fig. 3.

The contribution to $I(\Theta)$ by each of the potentials presented in Table I is shown in Fig. 4. The relative weights from Eq. (1) are used in the $I(\Theta)$ plots for all energies.

DISCUSSION

Dunning and Hay[3b] estimate the ionic contribution in configuration interaction to the $X\frac{1}{2}$ state to be 9.2% for XeF. However, the fact that their $X\frac{1}{2}$ potential does not well represent the $V_{X\frac{1}{2}}(r)$ given here and by Tellinghuisen et al.,[5c] raises the question of the accuracy of this appraisal. Yet, to simply say that the $X\frac{1}{2}$ binding is due to, or characterized by charge transfer, may be somewhat misleading. It is not clear that a two center coulombic interaction picture is really appropriate. For example, the role of inter-atomic correlation, and its coupling to intra-atomic correlation, formidable and important problems, need careful assessment. The $X\frac{1}{2}$ state is not strongly

bound by ordinary chemical standards, but it is significant that the $V_{X\frac{1}{2}}(r)$ minimum position, r_m, lies about 1½ Å inside the strictly van der Waals-like $V_{I\frac{3}{2}}(r)$ minimum. Though a physical picture of the electronic open shell-closed shell binding in the $X\frac{1}{2}$ state of XeF is not complete, the quantitative determination of $V_{X\frac{1}{2}}(r)$ carried out in this work is found, corroborating the spectroscopically derived potential by Tellinghuisen et al.

The estimates of the interaction potentials for the $I\frac{3}{2}$ and $II\frac{1}{2}$ states over the experimentally probed thermal energy range presented here should be quite realistic. At very small r, these two states should coalesce into a single $^2\Pi$ state as the electronic orbital angular momentum becomes strongly coupled to the internuclear axis, dominating the spin-orbit coupling.[3,24] However, these experiments at relatively low collision energies do not sample these internuclear distances, and the additional complication of including separate repulsive wall descriptions for the $V_{I\frac{3}{2}}(r)$ and $V_{II\frac{1}{2}}(r)$ is not warranted here.

ACKNOWLEDGEMENTS

We thank Drs. J. Tellinghuisen, T. H. Dunning and P. J. Hay for communicating their results to us prior to publication. This work was supported by the Office of Naval Research (Contract No. N14-77-C-0101). and by the Division of Chemical Sciences, U.S. Department of Energy. P.C. acknowledges a fellowship from the Italian National Research Council (CNR).

FOOTNOTES AND REFERENCES

*Permanent address: Dipartimento di Chimica dell' Università, 06100 Perugia, Italy.

†Guggenheim Fellow, 1977-1978.

1. For emission see e.g., (a) L. A. Kuznetsova, Y. Y. Kuzyakov, V. A. Shpanskii, and V. M. Khutoretskii, Vestn. Mosk. Univ. Ser. II Khim 19, 19 (1964); (b) M. F. Golde and B. A. Thrush, Chem. Phys. Lett. 29, 486 (1974); (c) J. E. Velazco and D. W. Sester, J. Chem. Phys. 62, 1990 (1975); (d) J. Tellinghuisen, A. K. Hays, J. M. Hoffman, and G. C. Tisone, J. Chem. Phys. 65, 4473 (1976). For laser action, see e.g., (e) S. K. Searles and G. A. Hart, Appl. Phys. Lett. 27, 243 (1975); (f) J. J. Ewing and C. A. Brau, Appl. Phys. Lett. 27, 350 (1975); (g) C. A. Brau and J. J. Ewing, Appl. Phys. Lett. 27, 435 (1975).

2. J. J. Ewing and C. A. Brau, Phys. Rev. A12, 129 (1975); J. Tellinghuisen, J. M. Hoffman, G. C. Tisone, and A. K. Hays, J. Chem. Phys. 64, 2484 (1976); M. Krauss, J. Chem. Phys. 67, 1712 (1977).

3. (a) P. J. Hay and T. H. Dunning, J. Chem. Phys. 66, 1306 (1977); (b) T. H. Dunning and P. J. Hay, "The covalent and ionic states of the rare gas monofluorides," J. Chem. Phys. (in press).

4. D. H. Liskow, H. F. Schaefer, P. S. Bagus, and B. Liu, J. Am. Chem. Soc. 95, 4056 (1973).

5. (a) J. Tellinghuisen, G. C. Tisone, J. M. Hoffman, and A. K. Hays, J. Chem. Phys. 64, 4796 (1976); (b) J. Tellinghuisen, P. C. Telling-

huisen, G. C. Tisone, J. M. Hoffman, and A. K. Hays, "Spectroscopic studies of diatomic noble gas halides III," J. Chem. Phys. (in press); (c) P. C. Tellinghuisen, J. Tellinghuisen, J. E. Velazco, J. A. Coxon, and D. W. Setser, "Spectroscopic studies of diatomic noble gas halides IV," J. Chem. Phys. (in press).

6. A. L. Smith and P. C. Kobrinsky, J. Mol. Spectr. 69, 1 (1978).

7. N. Bartlett and F. O. Sladky, Comprehensive Inorganic Chemistry, (Pergamon Press, London, 1973), Vol. I, p. 250.

8. H. S. Johnston and R. Woolfolk, J. Chem. Phys. 41, 269 (1964).

9. V. A. Legasov, V. N. Prusakov, and B. B. Chaivanov, Russ. J. Phys. Chem. 42, 610 (1968).

10. J. R. Morton and W. E. Falconer, J. Chem. Phys. 39, 427 (1963).

11. M. Krauss and B. Liu, Chem. Phys. Lett. 44, 257 (1976).

12. P. E. Siska, J. M. Parson, T. P. Schafer, and Y. T. Lee, J. Chem. Phys. 55, 5762 (1971).

13. K. S. Pitzer and L. Brewer, Thermodynamics (McGraw-Hill, New York, 1961), Second edition, p. 672.

14. R. K. Preston, C. Sloane, and W. H. Miller, J. Chem. Phys. 60, 4961 (1974).

15. See, e.g., E. H. S. Burhop in Quantum Theory, D. R. Bates, editor (Academic Press, New York, 1961) Vol. I, Ch. 9. The elastic phase-shifts are calculated by Numerov integration for F + Xe at 2.11 kcal/mole collision energy; otherwise, JWKB phase-shifts are used in the fitting, though accuracy is checked by Numerov integration.

16. A somewhat similar situation is described by R. Düren, H. O. Hoppe, and H. Pauly, Phys. Rev. Lett. 37, 743 (1976).

17. C. Y. Ng, Y. T. Lee, and J. A. Barker, J. Chem. Phys. 61, 1996 (1974).

18. H. J. Werner and W. Meyer, Phys. Rev. A13, 13 (1976).

19. J. S. Cohen and R. T. Pack, J. Chem. Phys. 61, 2372 (1974).

20. C. Froese Fischer, At. Data 4, 301 (1972).

21. K. S. Pitzer, Adv. Chem. Phys. 2, 59 (1959).

22. Values for the fluorine atom permanent quadrupole moment are found in M. A. Gardner, A. M. Karo, and A. C. Wahl, J. Chem. Phys. 65, 1222 (1976), and F. H. Mies, Phys. Rev. A7, 942 (1973). The Xe polarizability is given in Ref. 19. The permanent quadrupole-induced dipole induction energy is calculated from J. O. Hirschfelder, C. F. Curtiss, and R. B. Bird, Molecular Theory of Gases and Liquids (Wiley & Sons, New York, 1954), p. 987.

23. W. R. Wadt, P. J. Hay, and L. R. Kahn, J. Chem. Phys. 68, 1752 (1978).

24. See, e.g., G. Herzberg, Spectra of Diatomic Molecules (Van Hostrand Reinhold Co., New York, 1950) second edition; or F. Masnou-Seeuws and R. McCarrol, J. Phys. B7, 2230 (1974).

TABLE I. XeF potential parameters.

		$X\frac{1}{2}$	$I\frac{3}{2}$, $II\frac{1}{2}$
ε	(kcal/mole)	3.359	0.16
r_m	(Å)	2.293	3.80
β_1		8.5	7.5
β_2		6.8	6.0
X_1		1.102	1.116
X_2		1.950	1.500
C_6	(kcal/mole·Å^6)	703.	750.
C_8	(kcal/mole·Å^8)	3740.	3740.

FIGURE CAPTIONS

Fig. 1. Laboratory angular distributions of scattered F for the $F(^2P) + Xe(^1S)$ system at three collision energies. Solid curves are calculated from best fit potentials of Table I, averaging over angular and velocity distributions of experimental conditions. Dashed curves show single Newton diagram calculations, averaging over experimental angular resolution.

Fig. 2. Sensitivity of calculated laboratory angular distributions of F from $F(^2P) + Xe(^1S)$ to given potentials. The $I(\Theta)$ are calculated according to Eq. (1) from: (a) $X\frac{1}{2}$, $I\frac{3}{2}$, and $II\frac{1}{2}$ potentials of Ref. 3b; (b) $X\frac{1}{2}$ potential of Table I, and $I\frac{3}{2}$ and $II\frac{1}{2}$ potentials of Ref. 3b; (c) $X\frac{1}{2}$ potential of Ref. 11, and $I\frac{3}{2}$ and $II\frac{1}{2}$ potentials of Table I. The data are shown for comparison.

Fig. 3. Interaction potentials of $F(^2P_{3/2}) + Xe(^1S_0)$; the solid line (——) represents present work (see Table I); × (TTVCS) from Ref. 5c; ○ (KL) from Ref. 11; □, Δ (DH) from Ref. 3b. Note the scale change at V(r) higher than 1 kcal/mole.

Fig. 4. Relative contribution to $I(\Theta)$ (single Newton diagram calculations) of each of the potentials of Table I at three collision energies according to Eq. (1).

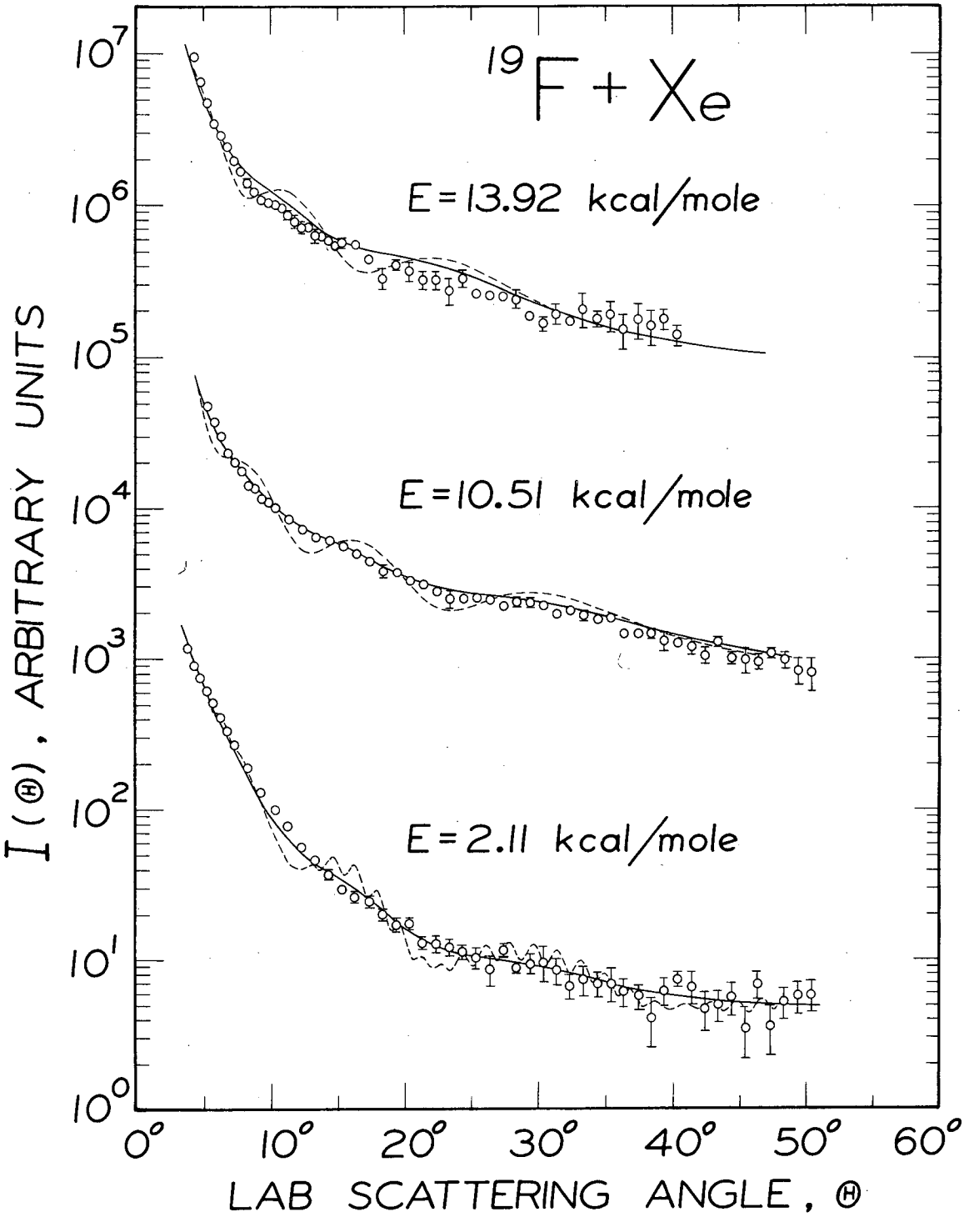

XBL 784-8182 A

Fig. 1

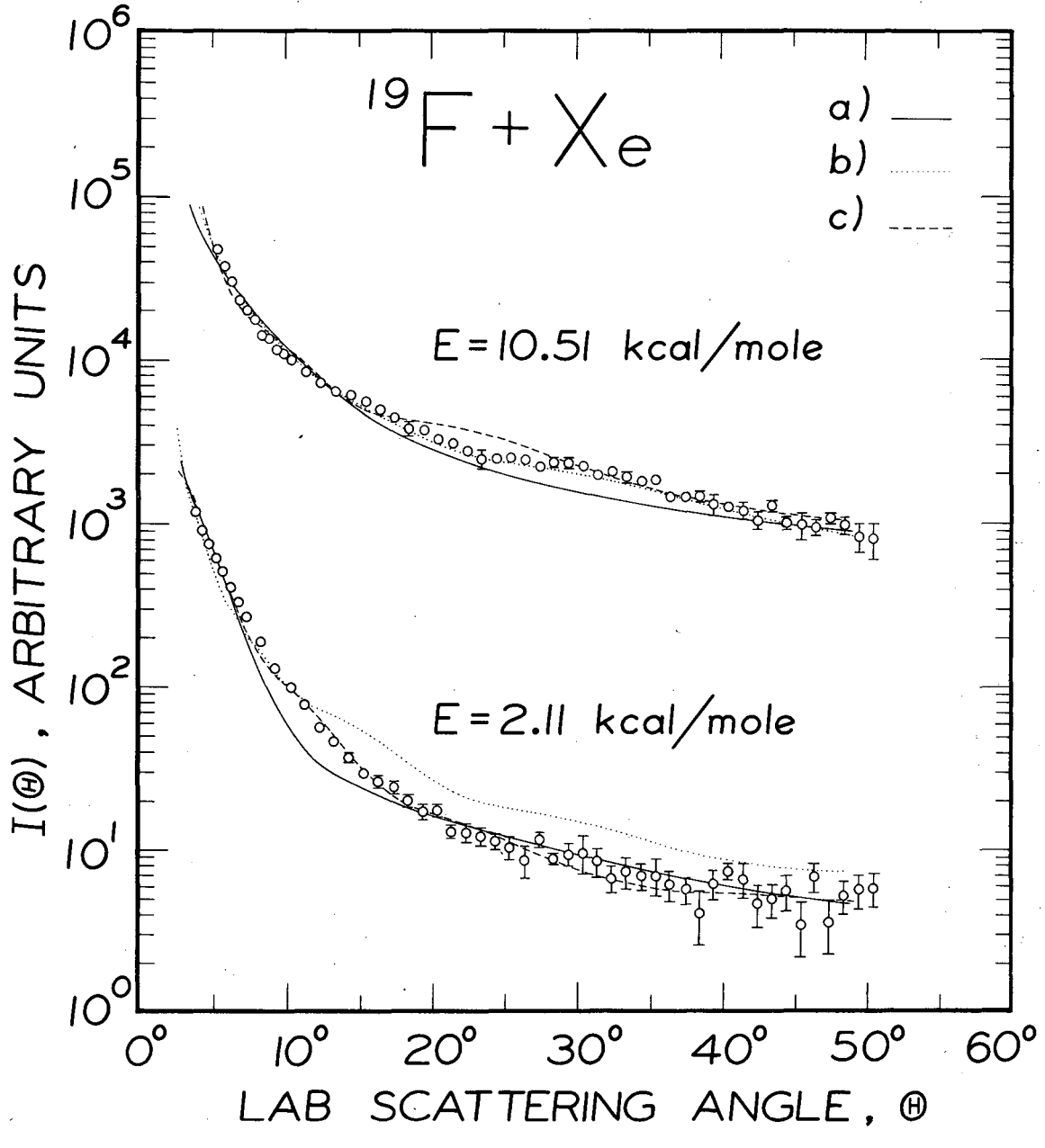
$^{19}F + Xe$
a)
b)
c)
E = 10.51 kcal/mole
E = 2.11 kcal/mole
I(Θ), ARBITRARY UNITS
LAB SCATTERING ANGLE, Θ
10^6
10^5
10^4
10^3
10^2
10^1
10^0
0°
10°
20°
30°
40°
50°
60°
XBL 784-8316

Fig. 2

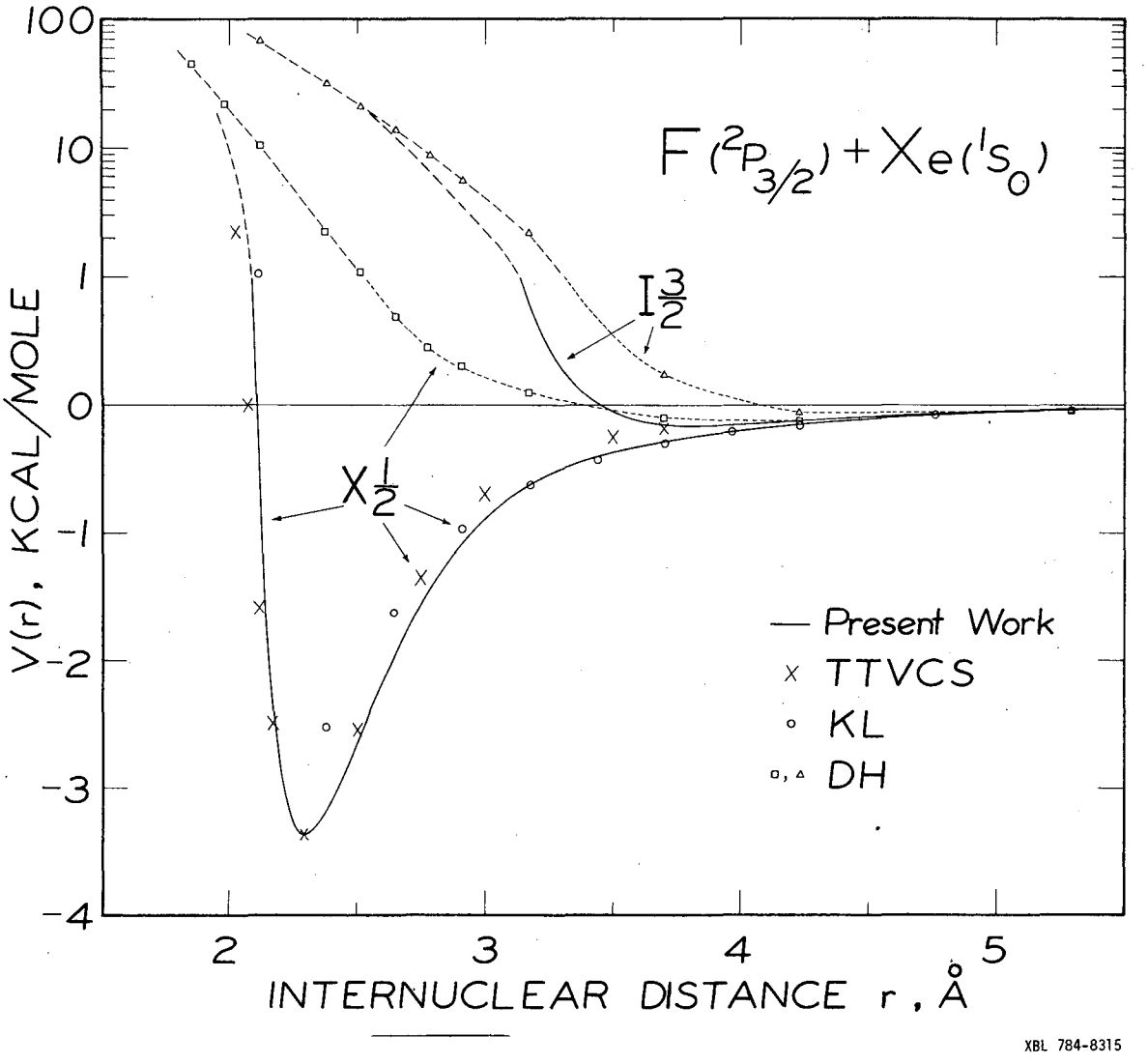

XBL 784-8315

Fig. 5

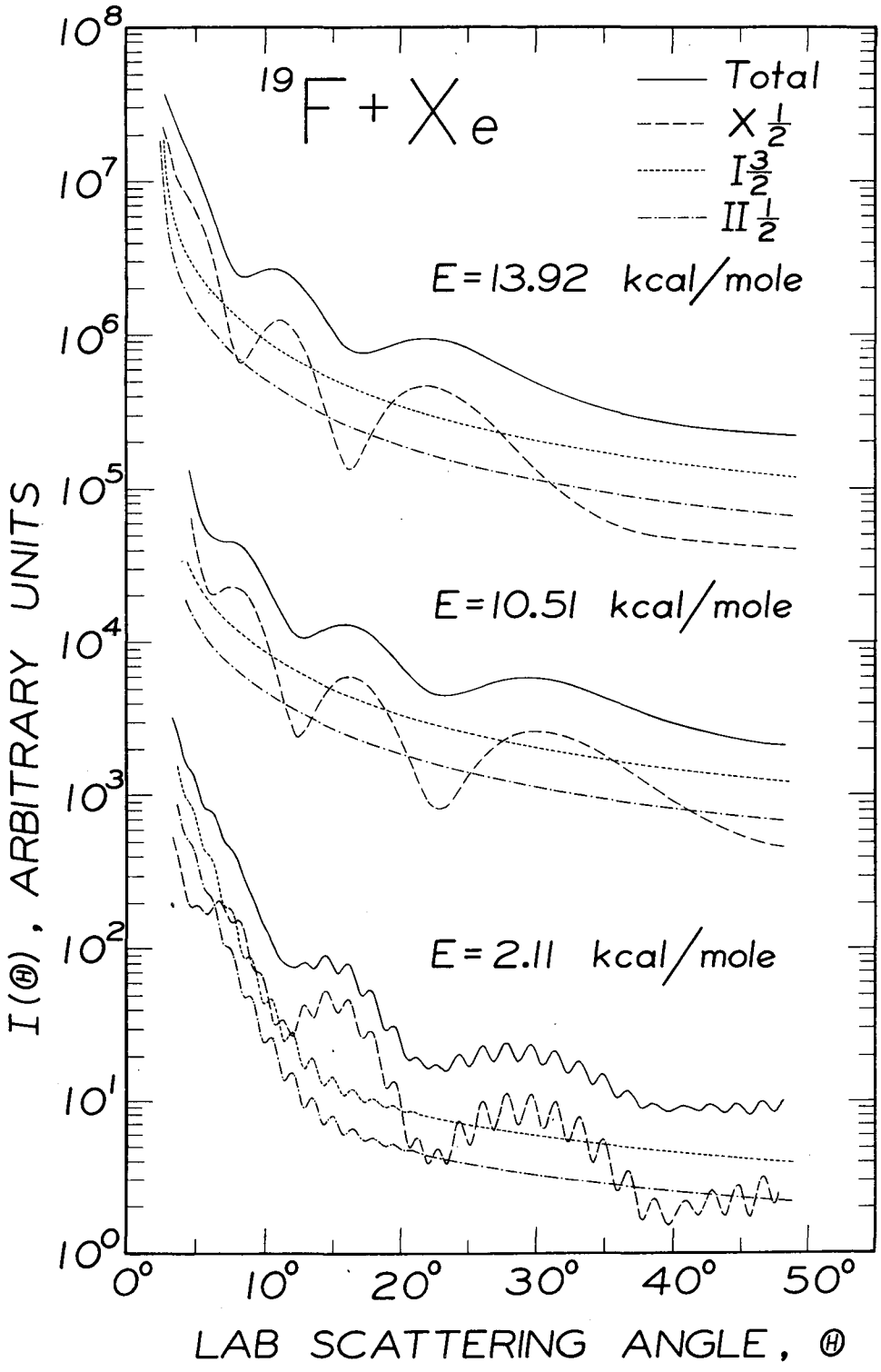

XBL 784-8382

Fig. 4

TECHNICAL INFORMATION DEPARTMENT
LAWRENCE BERKELEY LABORATORY
UNIVERSITY OF CALIFORNIA
BERKELEY, CALIFORNIA 94720